Int. J. Multiphase Flow Vol. 18, No. 4, pp. 577–592, 1992
Printed in Great Britain.

0301-9322/92 $5.00 + 0.00

ACOUSTIC WAVE SPEED AND ATTENUATION IN SUSPENSIONS

C. M. ATKINSON and H. K. KYTÖMAA
Department of Mechanical Engineering, Massachusetts Institute of Technology, Cambridge, MA 02139, U.S.A.

(Received 1 March 1991; in revised form 31 December 1991)

Abstract—Acoustic wave propagation in a monodisperse suspension of varying solids concentration was modeled exactly for wavelengths much larger than the particle size, including unsteady viscous effects, for the situation where particle interactions are predominantly inviscid. Inviscid particle interactions are addressed in terms of the added mass coefficient, which is sensitive to the solids concentration, the direction of insonification and the anisotropy of the particle arrangement. The sound speed and attenuation were calculated and compared to experimental results for a wide range of ka, where k is the wavenumber $(=2\pi/\lambda)$ and a is the particle radius. The attenuation, which is a strong function of ka, is seen to have non-monotonic behavior with respect to the solids fraction at low frequencies and it becomes monotonic at high frequencies. In general, the effect of ka on sound speed is seen to be small in comparison. The comparison with experiments shows that at values of ka near 1, effects associated with multiple scattering begin to affect acoustic propagation sufficiently to cause marked deviation between the present theory and measurements.

Key Words: suspensions, acoustic wave propagation, sound speed, attenuation

INTRODUCTION

Longitudinal acoustic waves travel through a single-phase fluid with a velocity that depends on the fluid density and compressibility. In suspensions and slurries, on the other hand, the wave speed is known to be dependent on the material properties of the two constituents as well as their relative concentrations. A simple phenomenological model for the speed of sound in a two-phase mixture, first proposed by Urick (1974), describes the inhomogeneous mixture in terms of its averaged density and compressibility. This "effective medium" model fits the available experimental data for the sound speed in suspensions very well for low non-dimensional acoustic wavenumbers $ka = 2\pi a/\lambda$, where a is an average radius of the particles in the suspension. The attenuation of sound in two-phase solid–liquid mixtures is known to increase with increasing frequency, but the dependence of attenuation on the dispersed phase concentration is less well known. It has been found experimentally that the acoustic attenuation of high frequency sound in suspensions of small particles (corresponding to low values of ka) is non-monotonic with respect to the concentration of solids in suspension—there is a distinct maximum in attenuation at an intermediate concentration between the dilute limit and the fully packed state (Urick 1948; Hampton 1967). This has important implications in the development of non-intrusive ultrasonic diagnostic techniques for the study of concentrated sprays, slurries, pastes and fluidized beds, only to mention a few examples, which cannot readily be probed with existing optical methods. Few attempts have been made to explain this behavior (Gibson & Toksöz 1989; Harker & Temple 1988), and by their assumptions, these models are restricted to low ka. In addition, they employ empirically motivated forms for the effective viscosity of the suspension and, in the case of the former treatment, steady drag behavior is assumed. As an extension of this previous work we develop the governing equations for the acoustics of suspensions to describe the behavior of sound in the inertially dominated acoustic regime of considerably higher ka than that studied previously.

There is a large body of literature on the propagation of acoustic waves in porous media, which has been motivated by seismological, oil exploration and oceanographical interests. However, acoustic wave propagation in porous media and suspensions, while similar, have important differences. For example, porous media exhibit elastic resistance to shear stresses (Biot 1956), while a suspension typically does not. Both, however, can sustain isotropic stresses. One of the difficulties

Table 1. Particle and fluid properties

	Hampton (1967)	Urick (1948)	This study
Experimental system	Kaolin/water	Kaolin/water	Silica/water
Frequency	100 kHz	1 MHz	100 kHz–1 MHz
Particle radius	1.0 μm	0.5 μm	0.5 mm
ka	$\sim 6.66 \times 10^{-5}$	$\sim 3.35 \times 10^{-4}$	$\sim$0.2 to 0.6

is in the representation of the relative motion between fluid and solids. In porous media this is described in terms of a frequency-dependent permeability, which has recently received attention (Attenborough 1983; Johnson *et al.* 1987): with a pore size, d, as a characteristic geometric length scale, if the viscous boundary layer thickness, $\delta(=\sqrt{2\mu/\rho_L\omega}$, where μ is the liquid viscosity, ρ_L is its density and ω is the angular frequency) is significantly greater than d, the permeability scales with viscosity and equals its steady flow value. On the other hand, if $d \gg \sqrt{2\mu/\rho_L\omega}$, the flow is essentially inviscid, is dominated by inertia and can be computed using potential theory. In the latter case, the dissipation is restricted to the thin boundary layer surrounding each particle. While similar scaling arguments can be made with suspensions, the analog of permeability is inherently coupled with the motion of the particles and cannot be described with linear elasticity. Below, the general solution of the Navier–Stokes equations to the problem of an oscillating sphere in a viscous fluid is generalized to accommodate oscillatory fluid motion, and it is included in the equations describing the acoustic behavior of a suspension. The sound speed and attenuation are then evaluated for the regime in which inertial effects dominate particle drag, and these predictions are then compared to experimental results.

Measurement of acoustic phase speed and attenuation

Results of the acoustic phase speed in suspensions reported by Hampton (1967) and Urick (1947, 1948) for $ka \sim O(10^{-5})$ and $O(10^{-4})$, respectively, bear out the utility of the phenomenological approach for small ka (see table 1). Here the wave speed c is given by

$$c = \sqrt{\frac{\bar{\kappa}}{\bar{\rho}}}, \qquad [1]$$

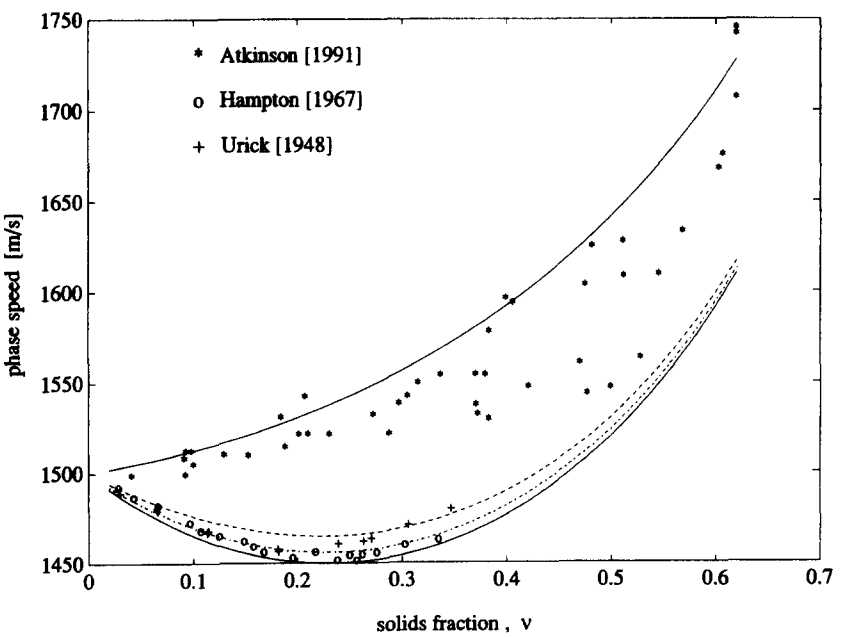

Figure 1. The variations of sound speed in a suspension with particle concentration: ○, $ka \simeq 6.6 \times 10^{-5}$ (Hampton 1967); +, $ka \simeq 3.4 \times 10^{-4}$ (Urick 1948). The data of Atkinson (1991) for $ka \simeq 0.2$ to 0.6 (*), show some scatter, but no minimum at intermediate solids fractions. The theoretical curves in ascending order are for ka values of 0, 6.66×10^{-5}, 3.4×10^{-4} and 0.2–0.6.

where the effective bulk modulus of the system is given by

$$\frac{1}{\bar{\kappa}} = \frac{v}{\kappa_s} + \frac{(1-v)}{\kappa_L} \quad [2]$$

and the suspension density is

$$\bar{\rho} = v\rho_s + (1-v)\rho_L. \quad [3]$$

The variables κ and ρ denote the bulk modulus and density of either the solid or the liquid according to the subscript s or L, respectively. For a system of silica particles in water, [1] predicts a minimum in sound speed at a solids fraction, v, of about 25–30%, and this prediction is borne out in the available experimental results at low ka. Results obtained by the present authors (figure 1), however, show differing behavior. For $ka \sim O(1)$, there is no minimum at intermediate concentrations and the velocity increases monotonically with concentration.

While the acoustic attenuation in concentrated suspensions is known to increase with frequency, the attenuations measured by Hampton (1967), Urick (1947, 1948) and the present authors show consistently non-monotonic behavior as a function of solids fraction or dispersed phase concentration, albeit for ka spanning 3–4 orders of magnitude (see, for example, figures 5, 6 and 8). By means of the analysis, it is later shown that the origin of the non-monotonic attenuation with respect to the solids fraction is different at high frequencies from that at low frequencies. We derive below a model to explain the respective behavior of attenuation and phase speed in suspensions for a wide range of frequencies up to $ka \approx 1$.

GOVERNING EQUATIONS

A two-component model for a suspension of monodisperse spheres in a Newtonian liquid is developed, and by performing a linear perturbation analysis, we derive the expected infinitesimal compressional wave speed as well as the wave attenuation in the composite medium.

The procedure for the formulation of the model is as follows: it is assumed that the solid particles as well as the liquid phase constitute a continuum. Once the two interacting continua assumption is made, a general continuity relation and a volume-averaged momentum balance for each of the two phases may be written. Thereafter, by invoking an equation of state for each phase, closure of the fluid dynamic equations is achieved.

For a solids fraction v of the total volume, the liquid phase continuity equation is

$$\frac{\partial(1-v)\rho_L}{\partial t} + \nabla[(1-v)\rho_L v_L] = 0, \quad [4]$$

where v_L is the liquid velocity. Similarly, the solid phase continuity equation takes the form

$$\frac{\partial v\rho_s}{\partial t} + \nabla[v\rho_s v_s] = 0, \quad [5]$$

where v_s is the solids velocity.

In developing the momentum conservation equations for high frequency acoustics in a concentrated mixture, it is helpful to evaluate the relative importance of viscous and inertial effects. It is shown below that inertial effects dominate the interface drag for the range of parameters of interest in the present study, i.e. large ka. For these the Reynolds number (Re) for oscillatory motion of a particle of radius a in a fluid of kinematic viscosity μ/ρ_L,

$$\mathrm{Re} = \sqrt{\frac{\rho_L \omega a^2}{2\mu}}, \quad [6]$$

is very high and it is evident therefore that the flow is essentially inviscid, with the exception of thin viscous boundary layers surrounding the particles. It is to these thin boundary layers that the viscous dissipation in the system is restricted. While they are discussed specifically below,

the appropriate form of the one-dimensional momentum equations, neglecting gravitational effects, is:

$$\rho_s v\left(\frac{\partial v_s}{\partial t}+v_s\frac{\partial v_s}{\partial x}\right)=F_{sL} \qquad \text{solids momentum} \qquad [7]$$

and

$$\rho_L(1-v)\left(\frac{\partial v_L}{\partial t}+v_L\frac{\partial v_L}{\partial x}\right)=-\frac{\partial P}{\partial x}+F_{Ls} \quad \text{liquid momentum.} \qquad [8]$$

The quantity P is the liquid static pressure. For the conditions of interest, where the bulk of the fluid behaves in an inviscid manner, viscous dissipation can be neglected outside the particle boundary layers, hence the absence of a $\mu\nabla^2 v_L$ term. In this analysis, we consider only viscous effects that arise due to interactions between the two phases. This effect appears in the momentum interaction term, F_{sL}, which is the force per unit volume imparted by the liquid on the solid. It is equal and opposite to F_{Ls}. Its specific form is developed in the section below.

Equations [4], [5], [7] and [8] represent 4 equations in 6 unknowns, v_L, v_s, ρ_L, ρ_s, P and v. In order to achieve closure of this set of equations, two equations of state that relate the density variation of each of the two phases to the pressure perturbation, P', are invoked, namely

$$\rho_L=\rho_L^0\left(1+\frac{P'}{\kappa_L}\right) \qquad [9]$$

and

$$\rho_s=\rho_s^0\left(1+\frac{P'}{\kappa_s}\right). \qquad [10]$$

The momentum interaction term F_{sL}

The momentum interaction force between the solid and the liquid, $F_{sL}=-F_{Ls}$, consists, in general, of dynamic drag (containing viscous and inertial effects) and buoyancy forces associated with the instantaneous liquid pressure gradient. In order to ascertain the momentum interaction force due to drag alone for a concentrated mixture, the single particle drag result must be extended to arbitrary concentrations of particles. Here, we develop a general extension of the exact solution for the unsteady motion of a single particle in a viscous fluid. To extend the single particle drag result to higher concentrations, we write the equivalent drag per unit volume, F_{eq}, for the suspension to be equal to the drag per sphere (in an assembly of spheres) multiplied by the number of spheres per unit volume, n, or $F_{eq}=nF_D$, where n can be written in terms of the solids fraction and particle radius:

$$n=\frac{3v}{4\pi a^3}. \qquad [11]$$

As was mentioned previously, there is also a component of the phase interaction force which is due to the instantaneous pressure gradients. This buoyancy force is included in the momentum interaction force between the phases in the following manner:

$$F_{Ls}=\frac{3vF_D}{4\pi a^3}+v\frac{\partial P}{\partial x}, \qquad [12]$$

where F_D is the unsteady force on a single sphere of radius a in an assembly of spheres executing oscillatory motion relative to the fluid.

Drag on an isolated sphere

The unsteady drag force on an isolated sphere, F_{D0}, was derived by Landau & Lifshitz (1982):

$$F_{D0}=6\pi\mu a\left(1+\frac{a}{\delta}\right)(v_s-v_L)+3\pi a^2\rho_L(\tfrac{2}{9}a+\delta)\frac{\mathrm{D}(v_s-v_L)}{\mathrm{D}t}, \qquad [13]$$

where

$$\frac{\mathrm{D}(v_s - v_L)}{\mathrm{D}t} = \left(\frac{\partial v_s}{\partial t} + v_s \frac{\partial v_s}{\partial x}\right) - \left(\frac{\partial v_L}{\partial t} + v_L \frac{\partial v_L}{\partial x}\right). \quad [14]$$

The specific form of this time derivative satisfies the condition of objectivity (Drew 1983). The parameter $\delta(=\sqrt{2\mu/\rho_L\omega})$ is the unsteady viscous boundary layer thickness surrounding the particle. Its dimension relative to the separation between nearest neighbors provides a measure of the importance of viscous effects. At low frequencies, δ is large, while the converse is true at high frequencies. For oscillatory, or harmonic, relative motion between the phrases, where $U_{rel} = v_s - v_L = U_0 e^{i\omega t}$, the drag force is given by

$$\begin{aligned} F_{D0} &= 6\pi\mu a U_{rel}\left(1 + a\sqrt{\frac{\rho_L}{2\mu}}\sqrt{\omega} + i\frac{a^2\rho_L}{9\mu}\omega + i\frac{a\rho_L}{2\mu}\sqrt{\frac{2\mu}{\rho_L}}\sqrt{\omega}\right) \\ &= 6\pi\mu a U_{rel}\left(1 + a\sqrt{\frac{\rho_L}{2\mu}}\sqrt{\omega} + ia\sqrt{\frac{\rho_L}{2\mu}}\sqrt{\omega} + i\frac{a^2\rho_L}{9\mu}\omega\right) \\ &= 6\pi\mu a U_{rel}\left(1 + \frac{a}{\delta} + i\frac{a}{\delta} + i\frac{2}{9}\frac{a^2}{\delta^2}\right). \end{aligned} \quad [15]$$

This implies that for $\delta \gg a$, or alternatively $R \ll 1$, the drag force reduces to the steady Stokesian drag, i.e. viscous forces dominate. On the other hand, for large ω, or $\delta \ll a$, the steady drag term becomes negligible compared to the dissipative term associated with the unsteady generation of vorticity in the boundary layer near the particle surface and its diffusion away from the particle surface. This latter limit shows the dominance of inertial forces [as manifested in the added mass term $i(2/9)(a^2/\delta^2)$] over viscous forces in the interphase drag. As will be seen later, it is the history force terms in the drag expression [the terms a/δ and $i(a/\delta)$] that contribute most significantly to the attenuation of acoustic waves in suspensions at high frequencies.

To give an indication of the regime of validity of each of the terms in the equation above, for a 1 mm particle in water the crossover frequency at which the steady viscous drag term (i.e. the ω^0 term) equals the transition terms (these contain δ^{-1}) is 0.25 Hz. Correspondingly, the second crossover frequency at which the ω^1 term (the inertial term) starts to dominate the drag is about 18 Hz. From this the following asymptotic behavior can be recognized. At very low ω, the expression reduces to the well-known steady Stokes drag result,

$$\lim_{\omega \to 0} F_{D0} = 6\pi\mu a(v_s - v_L); \quad [16]$$

and at high ω, the dominant term is

$$\begin{aligned} \lim_{\omega \to \infty} F_{D0} &= \tfrac{1}{2}\rho_L \frac{4\pi a^3}{3}\frac{\mathrm{D}(v_s - v_L)}{\mathrm{D}t} \\ &= C\rho_L \frac{4\pi a^3}{3}\frac{\mathrm{D}(v_s - v_L)}{\mathrm{D}t}, \end{aligned} \quad [17]$$

which can be recognized as the added mass term for the drag on an isolated sphere with an added mass coefficient, C of 1/2. So, clearly, for frequencies very much greater than the second crossover frequency (e.g. 1 kHz) it would seem appropriate to use the inertial asymptotic behavior of the drag law. However, while the drag becomes inertially dominated for high ω, the dissipation associated with the particle and fluid oscillation remains viscous in origin but is restricted to a boundary layer surrounding each particle that becomes thinner with increasing frequency of oscillation. As is shown below, for the case of $\omega > 100$ kHz, the terms that contain viscosity as a parameter have little effect on the sound speed, but do significantly affect the attenuation. While viscous interactions can be negligible at such high frequencies, potential interactions are not.

For comparison, the present equations are shown below with the added mass coefficient, in the limit of inviscid flow:

$$\frac{D_s v_s}{Dt}[\rho_s + C(v)\rho_L] - \frac{D_L v_L}{Dt}[C(v)\rho_L] = -\frac{\partial P}{\partial x} \quad [18]$$

and

$$\frac{D_L v_L}{Dt}\left[\rho_L + C(v)\rho_L\left(\frac{v}{1-v}\right)\right] - \frac{D_s v_s}{Dt}\left[C(v)\rho_L\left(\frac{v}{1-v}\right)\right] = -\frac{\partial P}{\partial x}. \quad [19]$$

These are consistent with the generally accepted form due to Jackson (1985) with regards to the added mass coefficient and they have the same form as those proposed by Wallis (1989), although therein the added mass coefficient is presented in terms of the variable β which is indicative of the quantity of fluid entrained by the moving solid.

The added mass term and its dependence on concentration

It has long been recognized that the added mass coefficient associated with each sphere in a suspension is a function of concentration as well as the geometrical configuration of the suspension. By analogy, this dependence is directly related to Maxwell's relation for the effective conductivity of such an assembly of non-conducting spheres in a conducting fluid. This analogy is appropriate as Laplace's equation governs both the electrical potential and potential flow. Maxwell (1881) obtained the following expression for β, the ratio of the liquid conductivity to that of the mixture for a *random* assembly of non-conducting spheres:

$$\beta = \frac{1 + \frac{v}{2}}{1 - v}. \quad [20]$$

This equation has been shown to be a good approximation up to maximum packing concentrations of monodispersed spheres (Turner 1976). In the theory of inviscid multicomponent flows due to Wallis (1989), his equations of motion [(3.52) and (3.53)] lead to the following expression for the added mass coefficient:

$$C(v) = \left(\frac{1-v}{v}\right)[(1-v)\beta - 1], \quad [21]$$

where β is a factor by which the flux of the fluid is reduced due to the presence of the particles. Using Maxwell's form of β, the added mass coefficient reduces to a simple function of the solids fraction:

$$C(v) = \left(\frac{1-v}{2}\right), \quad [22]$$

which is used in F_{sL} to account for potential interactions. This expression for the added mass assumes the correct value of 1/2 at zero concentration. It must be remembered here that this coefficient is very sensitive to the geometrical configuration (which explains the differences between existing models) and that this chosen representation is strictly valid for random distributions of monodisperse spheres. The general form of the unsteady drag in the absence of viscous interactions, and including inviscid interactions, thus takes the form

$$F_D = 6\pi\mu a\left(1 + \frac{a}{\delta}\right)(v_s - v_L) + \tfrac{4}{3}\pi a^3 \rho_L\left[C(v) + \frac{9\delta}{4a}\right]\frac{D(v_s - v_L)}{Dt}. \quad [23]$$

Limits of validity

The condition where there are no viscous interactions between particles, while potential interactions may exist, is ubiquitous for high frequency ultrasonic applications with non-Brownian particles, and it requires that the viscous boundary layers (of thickness δ) surrounding adjacent

particles must not overlap. This is satisfied in the limit that $\delta \ll h/2$, where h is the average inter-particle spacing, which is strongly concentration dependent. Now, from geometrical arguments, h is given by

$$\frac{h}{a} = \frac{1 - \eta^{1/3}}{\eta^{1/3}}, \qquad [24]$$

where

$$\eta = \frac{\nu}{\nu_{max}} \qquad [25]$$

and the maximum particle packing fraction $\nu_{max} \simeq 0.635 \pm 0.005$ for a random close-packed structure of monodisperse spheres and $\nu_{max} \simeq 0.555$ for random loose packing (Onoda & Liniger 1990).

The requirement for no viscous interactions implies that the frequencies for which the present theory is valid are such that

$$\omega \gg \frac{4\mu}{a^2 \rho_L} \left[\frac{\eta^{2/3}}{(1 - \eta^{1/3})^2} \right]. \qquad [26]$$

This constraint is tantamount to neglecting the effects encountered in hindered viscous settling. The regime of ω and ν for which this restriction holds in a suspension of particles of radius 0.5 mm in water is shown in figure 2.

A complete set of equations has now been developed, and their limits of validity have clearly been investigated. Continuity is imposed by [4] and [5], which, with the equations of state [9] and

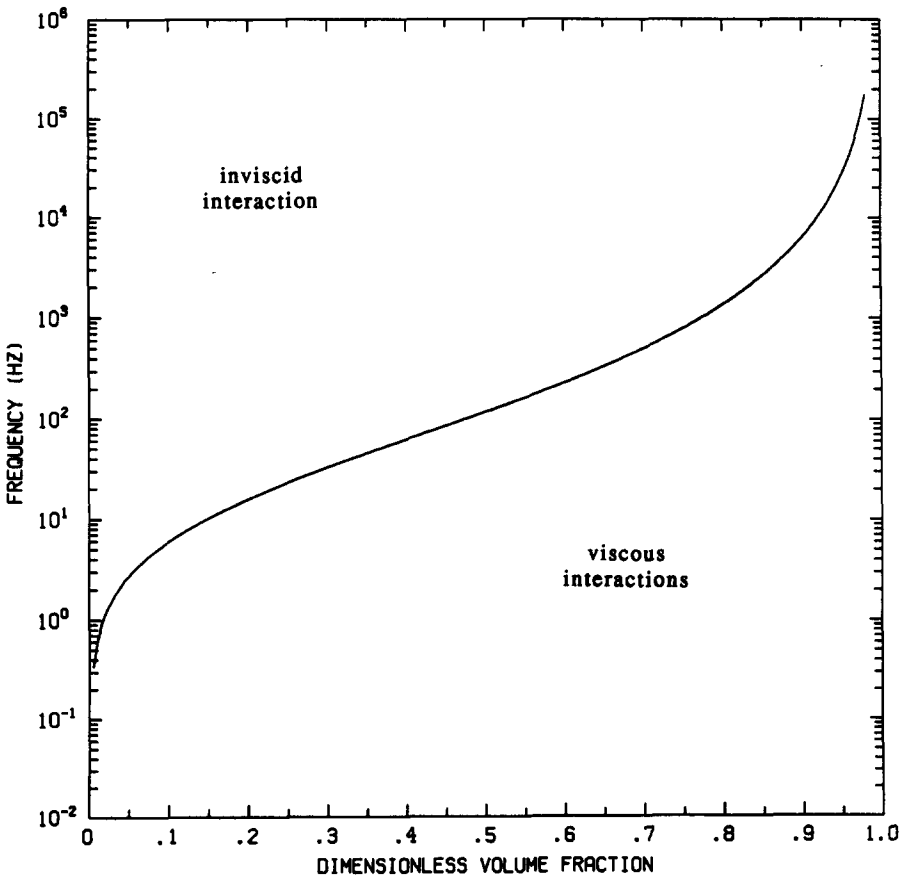

Figure 2. Regime map to identify the presence or absence of viscous particle interactions in terms of frequency and dimensionless solids fractions (ν/ν_{max}). For frequencies above this curve, the 0.5 mm particles (in water) may be considered to have non-overlapping viscous boundary layers.

[10], allow for the compressibility of the materials. In the context of the present long-wavelength theory, resonance effects in the solids are not relevant, and have for this reason been omitted from the discussion. Linear momentum is conserved by [7] and [8], which draw upon [12] and [23] for the form of the frequency- and concentration-dependent momentum interaction term. The generality and validity of this term over a vast range of frequencies and solids fractions and its ability to capture both viscous and inviscid behavior for the stated range is the principal analytical contribution of this theory in comparison with past efforts. Below, these equations are linearly perturbed, and traveling wave solutions are presented in terms of phase speed and attenuation.

LINEARIZED EQUATIONS

We assume that the state variables v_L, v_s, P, ν, ρ_L and ρ_s (denoted collectively by $f = f^0 + f'$) are perturbed from their steady state values by some small amount. The frequencies of excitation of the particles in the fluid due to the acoustic wave propagation are sufficiently high that the time scale of the duration of an individual wave or a series of waves is very much smaller than the time scale for any other fluctuation in the flow. This implies that the motion of the particle due to its oscillation in the sound wave may be completely decoupled from its gross motion in whatever flow situation is being considered, be it flow in a pipeline or in a fluidized bed. The time-averaged velocity of the particles and the liquid may be taken to be zero, or

$$v_L^0 = v_s^0 = 0. \tag{27}$$

Likewise, the datum pressure may be arbitrarily assumed to be zero or

$$P^0 = 0. \tag{28}$$

Our state variables thus reduce to

$$\begin{bmatrix} v_L \\ v_s \\ P \\ \nu \\ \rho_L \\ \rho_s \end{bmatrix} = \begin{bmatrix} v_L' \\ v_s' \\ P' \\ \nu^0 + \nu' \\ \rho_L^0 + \rho_L' \\ \rho_s^0 + \rho_s' \end{bmatrix}. \tag{29}$$

The linearized perturbation equations are (to first order in the perturbed variables):

$$\frac{\partial(1-\nu^0)\rho_L'}{\partial t} - \frac{\partial \rho_L^0 \nu'}{\partial t} + \frac{\partial(1-\nu^0)\rho_L^0 v_L'}{\partial x} = 0, \tag{30}$$

$$\frac{\partial \nu^0 \rho_s'}{\partial t} + \frac{\partial \rho_s^0 \nu'}{\partial t} + \frac{\partial \nu^0 \rho_s^0 v_s'}{\partial x} = 0, \tag{31}$$

$$\rho_L^0(1-\nu^0)\left(\frac{\partial v_L'}{\partial t}\right) = -(1-\nu^0)\frac{\partial P'}{\partial x} + \frac{9\mu\nu^0}{2a^2}\left(1+\frac{a}{\delta}\right)(v_s' - v_L') + \frac{9\nu^0}{4a}\rho_L'\left[\tfrac{4}{9}C(\nu^0)a + \delta\right]\left(\frac{\partial v_s'}{\partial t} - \frac{\partial v_L'}{\partial t}\right), \tag{32}$$

$$\rho_s^0 \nu^0 \left(\frac{\partial v_s'}{\partial t}\right) = -\nu^0 \frac{\partial P'}{\partial x} - \frac{9\mu\nu^0}{2a^2}\left(1+\frac{a}{\delta}\right)(v_s' - v_L') - \frac{9\nu^0}{4a}\rho_L'\left[\tfrac{4}{9}C(\nu^0)a + \delta\right]\left(\frac{\partial v_s'}{\partial t} - \frac{\partial v_L'}{\partial t}\right), \tag{33}$$

$$\rho_L' = \frac{\rho_L^0 P'}{\kappa_L} \tag{34}$$

and

$$\rho_s' = \frac{\rho_s^0 P'}{\kappa_s}. \tag{35}$$

DISPERSION RELATION

We seek wave-like solutions to these equations of the form

$$f' = f^0 e^{i(\omega t + kx)}, \tag{36}$$

where

$$k = \frac{\omega}{c} + i\alpha, \tag{37}$$

c is the wave speed in the medium and α is the attenuation parameter. Substituting the perturbed variables into the full equations and neglecting terms higher than first order in the perturbation variables, we obtain the following matrix equation:

$$[\mathbf{M}] \begin{bmatrix} v_L' \\ v_s' \\ P' \\ v' \\ \rho_L' \\ \rho_s' \end{bmatrix} = \mathbf{0}, \tag{38}$$

where

$$\mathbf{M} = \begin{bmatrix} -A - i\omega B & A + i\omega(B + \rho_s^0) & ik & 0 & 0 & 0 \\ A + i\omega\left[B + \rho_L^0\left(\frac{q - v^0}{v^0}\right)\right] & -A - i\omega B & ik\left(\frac{1 - v^0}{v^0}\right) & 0 & 0 & 0 \\ k\rho_L^0(1 - v^0) & 0 & 0 & -\omega\rho_L^0 & \omega(1 - v^0) & 0 \\ 0 & k\rho_s^0 v^0 & 0 & \omega\rho_s^0 & 0 & \omega v^0 \\ 0 & 0 & -\frac{\rho_L^0}{\kappa_L} & 0 & 1 & 0 \\ 0 & 0 & -\frac{\rho_s^0}{\kappa_s} & 0 & 0 & 1 \end{bmatrix},$$

where

$$A = \frac{9\mu}{2a^2}\left(1 + \frac{a}{\delta}\right) \tag{39}$$

and

$$B = \rho_L\left[C(v^0) + \frac{9}{4}\frac{\delta}{a}\right]. \tag{40}$$

This implies that the column vector has a non-trivial solution iff

$$\det \mathbf{M} = 0; \tag{41}$$

which in turn implies that

$$k^2 = \frac{\omega^2}{\bar{\kappa}} \frac{[(A + i\omega B)\bar{\rho} + i\omega\rho_s\rho_L(1 - v)]}{A + i\omega B + i\omega(1 - v)\rho^*}, \tag{42}$$

where

$$\rho^* = (1 - v)\rho_s + v\rho_L \tag{43}$$

and $\bar{\kappa}$ and $\bar{\rho}$ are defined by [2] and [3], respectively. The phase speed c is given by

$$c = \frac{\omega}{\Re(k)} \tag{44}$$

and the attenuation by

$$\alpha(\omega) = \Im(k); \tag{45}$$

$\Re(\ )$ and $\Im(\ )$ denote the real and imaginary parts of the argument.

The above equations can readily be used to compute the sound speed and attenuations for the full range of relevant frequencies. The square root prevents further algebraic simplification, although, for most applications it can easily be verified that within the assumptions already made, the real part of k will typically be much larger than its imaginary part by two or more orders of magnitude. If the condition

$$|\Im(k)| \ll |\Re(k)| \tag{46}$$

applies, the real and imaginary parts of k can be written as

$$\Re(k) \simeq \sqrt{\Re(k^2)}. \tag{47}$$

Now

$$\Im(k^2) = 2\Re(k)\Im(k) \tag{48}$$

or

$$\Im(k) \simeq \frac{\Im(k^2)}{2\sqrt{\Re(k^2)}}, \tag{49}$$

and the real and imaginary parts of k^2 are given by

$$\Re(k^2) = \frac{\omega^2}{\bar{\kappa}} \frac{A^2\bar{\rho} + \omega^2[B + (1-\nu)\rho^*][B\bar{\rho} + \rho_s\rho_L(1-\nu)]}{A^2 + \omega^2[B + (1-\nu)\rho^*]^2} \tag{50}$$

and

$$\Im(k^2) = \frac{\omega^2}{\bar{\kappa}} \frac{A\omega(1-\nu)(\rho_s\rho_L - \bar{\rho}\rho^*)}{A^2 + \omega^2[B + (1-\nu)\rho^*]^2}. \tag{51}$$

These equations are used below to present the asymptotic behavior of the sound speed and attenuation in the limits of $\omega \to \infty$ and $\omega \to 0$.

RESULTS

Sound speed

The computed sound speed is shown in figure 3 for a range of Re to demonstrate that it assumes constant values in the viscous and inviscid limits. This figure clearly shows the demarcation between the two regimes at $\mathrm{Re} \sim 100$. The low frequency limit for the sound speed as predicted by the two-component model is given by

$$\lim_{\omega \to 0} c = \left(\frac{\bar{\kappa}}{\bar{\rho}}\right)^{1/2}, \tag{52}$$

which is entirely independent of the frequency and material properties other than the fluid and solid densities and compressibilities. In the limit that $ka \to 0$, the sound speed as a function of ka reduces to that predicted by the phenomenological model of Urick (1947) (figure 1). In addition, the low frequency expression has the expected behavior for the high and low concentration limits: for $\nu \to 0$, or pure fluid, the velocity tends to that of the single-phase fluid,

$$c = \left(\frac{\kappa_L}{\rho_L}\right)^{1/2}. \tag{53}$$

The high frequency limit for the sound speed is given by

$$\lim_{\omega \to \infty} c = \left\{\frac{\bar{\kappa}\left[C + \dfrac{(1-\nu)\rho^*}{\rho_L}\right]}{C\bar{\rho} + (1-\nu)\rho_s}\right\}^{1/2}. \tag{54}$$

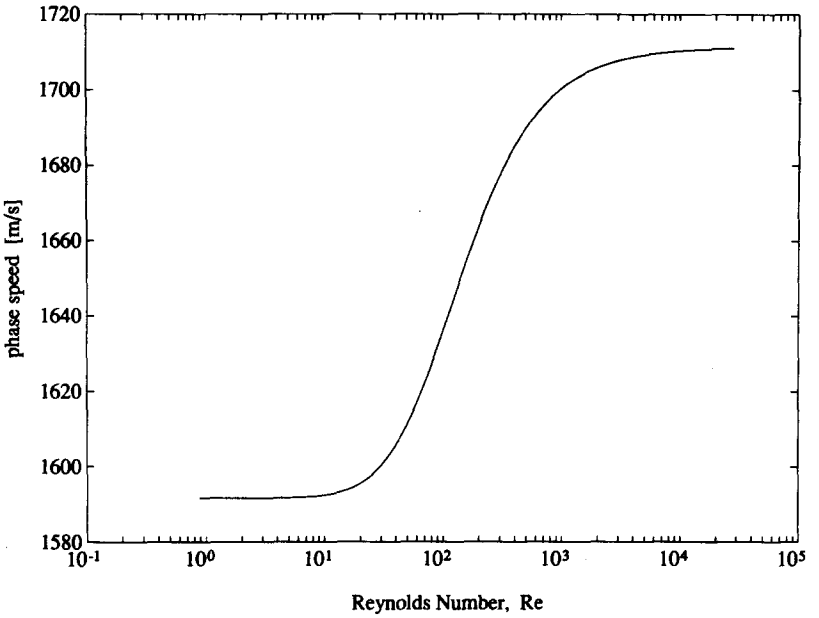

Figure 3. Theoretical sound speed as a function of Re for silica particles in water at a concentration of 60%. For $\mathrm{Re} \to 0$, the sound speed tends to the prediction of the phenomenological model of Urick (1947); and for $\mathrm{Re} \gg 100$, the sound speed asymptotes to a value somewhat greater than the speed in pure water.

Note that the viscosity is absent from the sound speed at high frequencies and does not physically affect it. As was pointed out briefly earlier, the added mass coefficient C is not only concentration dependent, but it is also highly sensitive to orientation if the particle is anisotropic, as is the case with fibers. Therefore from [54], it is reasonable to expect orientation and isotropy to affect speed. However, closer scrutiny will reveal that both the numerator and the denominator are dependent on C to the first order and, as a result, the sound speed is relatively insensitive to local microstructure. The phase velocity of a compressional wave in a suspension as defined by [42] and [44] is compared to the available data for a range of ka in figure 1. For $ka \sim O(1)$, the sound speed

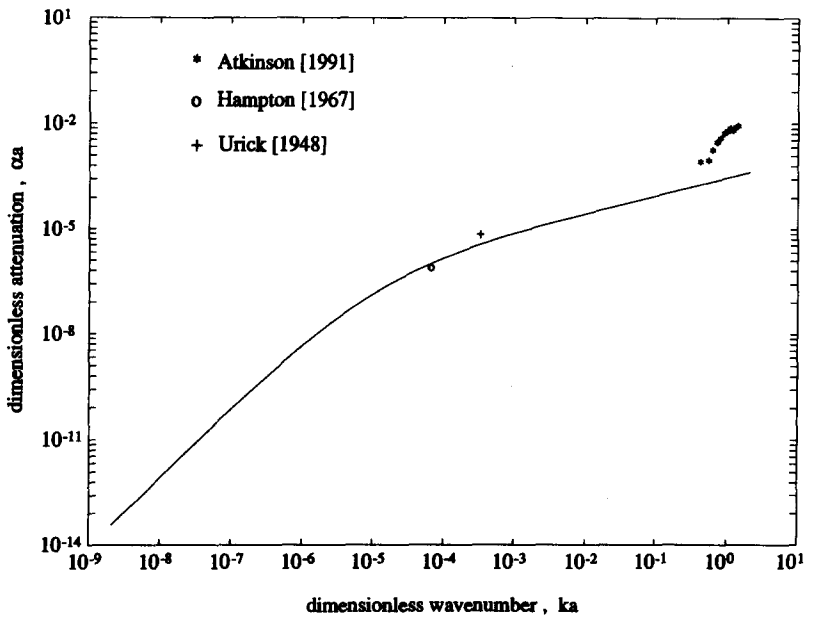

Figure 4. Dimensionless representation of the acoustic attenuation αa as a function of ka at a solids fraction of 60%; ○, Hampton (1967); +, Urick (1948); *, Atkinson (1991). The data spans 4 orders of magnitude of ka.

profile can be seen to be somewhat different from the low frequency case, and does not show a minimum at intermediate concentrations, but rather increases monotonically with increasing solids fraction. The difference in the behavior of c across four orders of magnitude of ka is not large, and the sound speed thus shows a relative insensitivity to frequency and all other factors except the fluid and particle densities and compressibilities. This is an important point in the context of on-going studies associated with the diagnosis of internal structure and anisotropy. The above results suggest that it may be difficult to infer anisotropy and internal structure from sound speed measurements alone, since the effect is of the order of the accuracy of typical measurements.

Attenuation

The attenuation predicted by [42] and [45], plotted in figure 4 as the continuous curve, exhibits a clear change in slope which separates the viscous and inviscid regimes. In the low frequency limit where viscous effects dominate, the attenuation is predicted to be

$$\lim_{\omega \to 0} \alpha = \frac{a^2\omega^2}{9\mu}(1-v)\frac{(\rho_s\rho_L - \rho^*\bar{\rho})}{\bar{\kappa}^{1/2}\bar{\rho}^{1/2}}, \qquad [55]$$

and is found to be proportional to ω^2. It should be noted here that as this expression is for the range of frequencies for which viscous particle interactions are significant, and as these are presented in the simpler form of isolated particles, the v dependence in the above equation is not expected to be correct. Unlike the form used for this regime, the Stokes drag and the Basset history terms are expected to generally be concentration dependent, as has been shown in numerous hindered viscous settling studies. The resulting attenuation is therefore inaccurate in magnitude. However, as the model contains all the appropriate physical ingredients, the quadratic frequency dependence is unaffected by the use of concentration-independent rather than concentration-dependent drag terms.

It is interesting to observe that in the viscous regime, the attenuation of sound scales inversely with viscosity, which suggests that at low frequencies, good penetration can readily be achieved with pastes and other thick mixtures.

There are few reported sets of data in the literature that show attenuation in suspensions. The data that are available for frequencies that straddle the viscous and the inviscid regimes show a distinct maximum at intermediate concentrations. See figure 5 [from Hampton (1967)] for

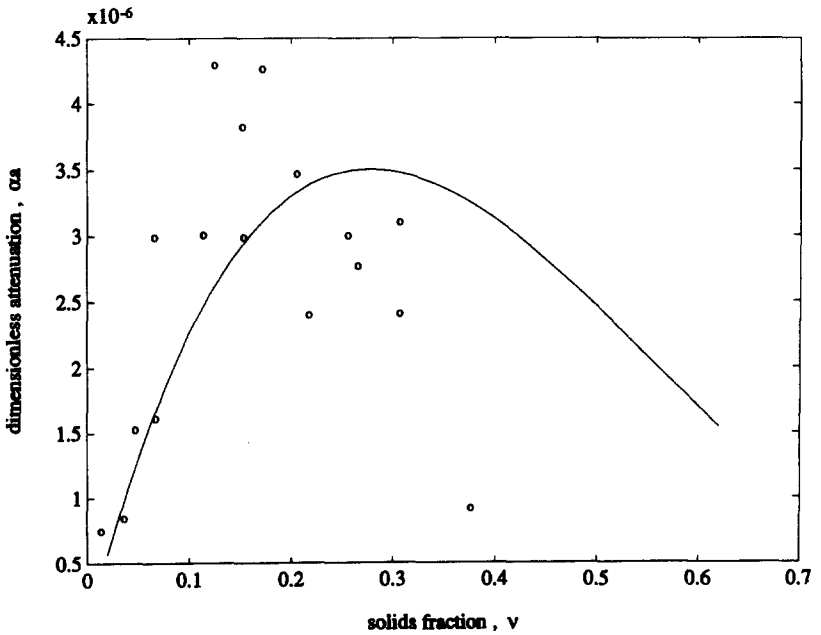

Figure 5. Dimensionless attenuation (αa) as a function of solids fraction for $ka = 6.7 \times 10^{-5}$ for a kaolinite particle suspension in water (Hampton 1967). The continuous curve is the theoretical prediction.

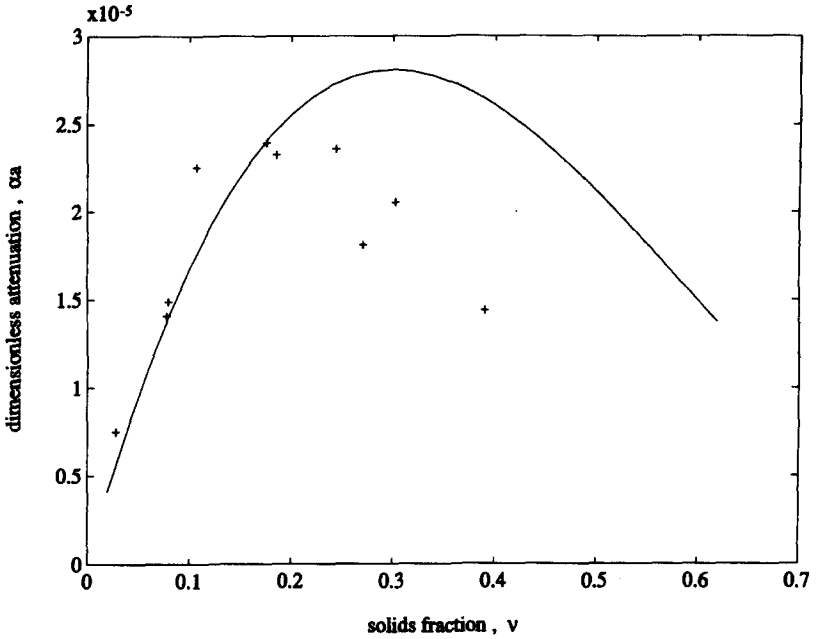

Figure 6. Dimensionless attenuation (αa) as a function of solids fraction for $ka = 3.4 \times 10^{-4}$ for a kaolinite particle suspension in water. The continuous curve is the theoretical prediction.

$ka \simeq 6.66 \times 10^{-5}$ and figure 6 [from Urick (1948)] for $ka \simeq 3.4 \times 10^{-4}$. This feature is clearly borne out in the simulations.

At high frequencies the attenuation is given by

$$\lim_{\omega \to \infty} \alpha = \frac{9}{4a} \sqrt{\frac{\mu\omega}{2\bar{\kappa}}} \frac{(1-v)(\rho_s \rho_L - \rho^* \bar{\rho})}{[\bar{\rho}C + \rho_s(1-v)]^{1/2}[\rho_L C + \rho^*(1-v)]^{3/2}}. \quad [56]$$

This leads to the result that the attenuation is proportional to $(\mu\omega)^{1/2}$, which is consistent with the Biot (1956) theory. As $\mu \to 0$, the attenuation tends to zero, which is to be expected as the

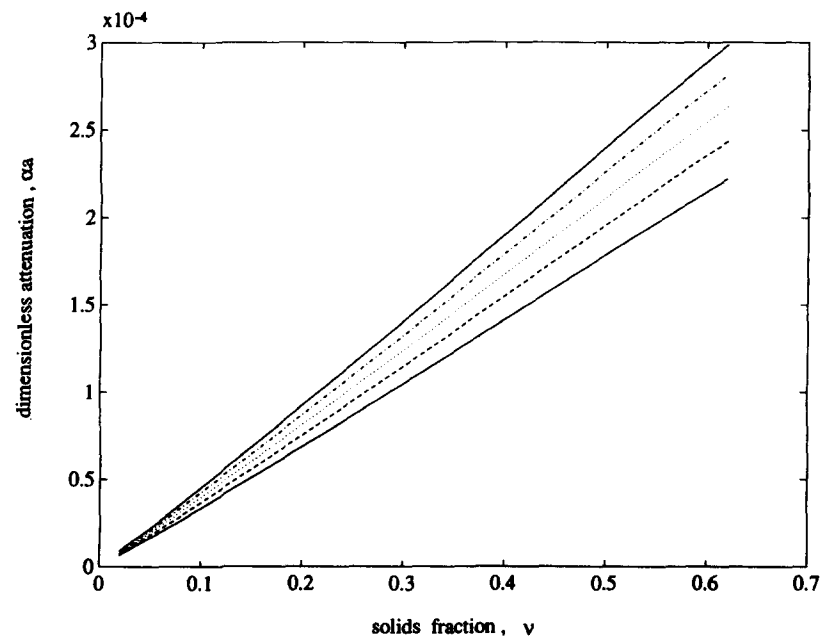

Figure 7. Theoretical dimensionless attenuation αa in a suspension of 0.5 mm radius silica particles in water as a function of solids concentration (Atkinson 1991) according to the long-wavelength theory. Data are in ascending order for $ka = 0.52$ (————), 0.62 (– – –), 0.73 (· · · ·), 0.84 (–·–·–), 0.94 (————).

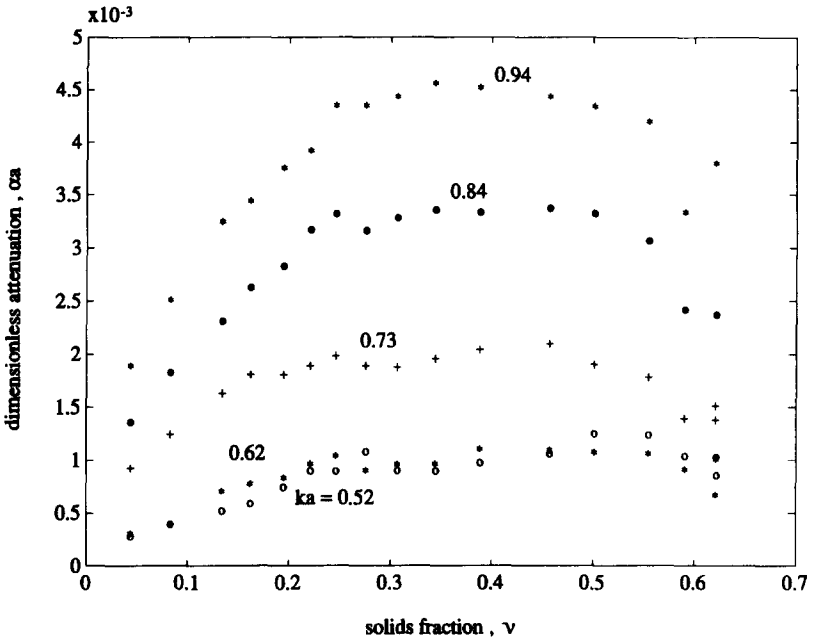

Figure 8. Dimensionless attenuation for αa acoustic wave propagation in a suspension of 0.5 mm radius silica particles in water as a function of solids concentration (Atkinson 1991). Data are in ascending order for $ka = 0.52$ (○), 0.62 (*), 0.73 (+), 0.84 (●), 0.94 (*).

dissipation is purely viscous in nature, although it should be noted that the chief attenuation mechanism is not viscous forces arising from the steady or Stokesian drag, but viscous interactions due to the Basset or history terms that dominate drag losses at high frequencies of oscillation. Calculated attenuations for the high frequency regime are plotted in figure 7 for $ka \simeq 0.5$ to 1.0. These results have a distinct monotonic linear character, unlike their lower frequency counterparts. Experiments conducted by Atkinson (1991) to verify this (figure 8) exhibit attenuations that are an order of magnitude higher than the theory and that behave in a marked non-monotonic fashion similar to that found at intermediate frequencies. This data clearly illustrates the limits of the current theory. As $ka \to 1$, geometric and multiple scattering effects, which are unaccounted for in this theory become increasingly important.

The attenuation has been shown to vary much more than the sound speed, not only between regimes but also within the viscous and inviscid regimes. This sensitive behavior is also observed as ka begins to encroach upon the multiple scattering regime. At $ka \sim O(1)$, the sound speed exhibits no discernible change while the attenuation is up to an order of magnitude greater than the theoretical predictions of the long-wavelength theory. This further emphasizes the value in conducting attenuation or signal amplitude measurements to obtain sensitive information regarding the microstructure of a mixture.

DISCUSSION

We have presented a theory of acoustic wave propagation in suspensions for a range of the non-dimensional wavenumber ka of approx. 4 orders of magnitude, spanning both the viscous and inviscid regimes up to but not including multiple scattering regime. In comparisons with experiments, existing data show good agreement with this model. It was shown that the attenuation of acoustic waves propagating in a suspension of monodisperse spheres in a viscous fluid at high frequency is primarily due to the Basset or history effects associated with the oscillatory relative motion between the particles and the fluid. At low frequencies of oscillation corresponding to large boundary layer thicknesses relative to the particle radius, the chief attenuation mechanism is steady or Stokesian drag on the particles. In contrast to the large observed variations in attenuation over the range of frequencies considered, the effect of frequency on the speed of sound is small.

In the high frequency limit, the present theory predicts the attenuation to scale with $(\mu\omega)^{1/2}$, which is consistent with the Biot (1956) theory. This power law has also been confirmed experimentally by Salin & Schön (1981).

At $ka \approx 1$, it has been found experimentally (Atkinson 1991) that the attenuation deviates from the 1/2 power law and assumes a higher power dependence with frequency (figure 4). This is probably due to multiple scattering effects which are known to dominate the attenuation behavior of suspensions at high frequencies (Allegra & Hawley 1971; Waterman & Truell 1961). Multiple scattering effects are also known to occur in porous media at $kd \sim 1$, where d is some representative pore size (Salin & Schön 1981). As a rule of thumb, the high ka data in figure 4 suggest that only for $ka < 0.1$ will the attenuation be relatively free of multiple scattering effects, although operation at higher frequencies is certainly possible with tolerable attenuation, to a point. It is further observed that in the inertial regime, while the theoretical attenuation becomes linearly proportional to concentration, the experiments for $ka \sim O(1)$ were found to significantly deviate from this, exhibiting non-monotonic behavior and values of αa much larger than predicted. This is suspected to be related to the same observed incipient multiple scattering effects.

In summary, for all ka up to $\sim O(1)$ the primary attenuation mechanism for acoustic wave propagation in a particular suspension appears to be the viscous interactions due to steady drag and Basset or history forces between the oscillating fluid and the particles. At frequencies that correspond to viscous boundary layer thicknesses of the order of the particle diameter, the attenuation exhibits a distinct peak at intermediate concentrations, and proves to penetrate dense suspensions much better than dilute ones. This has encouraging practical consequences in the use of ultrasound with concentrated slurries. In the inertial regime, the peak in attenuation soon disappears upon a small increase in frequency, and gives way to a monotonic dependence upon concentration. In this regime, there is an increase in sensitivity to microstructure. This provides an avenue for implementation of acoustic methods for particle geometry and particle alignment diagnostics. As $ka \to 1$, measured attenuation exhibit significant deviation from the theory and begin to grow prohibitively rapidly, resulting in progressively poorer penetration. This is the limit of the theory beyond which the long-wavelength assumption is no longer valid.

Acknowledgement—The authors are grateful for the support of the NSF under Grant Nos MSM-8809233 and CTS-9007496.

REFERENCES

ALLEGRA, J. R. & HAWLEY, S. A. 1971 Attenuation of sound in suspensions and emulsions: theory and experiments. *J. Acoust. Soc. Am.* **51,** 1545–1564.

ATKINSON, C. M. 1991 Acoustic wave propagation and non-intrusive velocity measurements in suspensions. Ph.D. Thesis, MIT, Cambridge, MA.

ATTENBOROUGH, K. 1983 Acoustical characteristics of rigid fibrous absorbents and granular materials. *J. Acoust. Soc. Am.* **73,** 785–799.

BIOT, M. 1956 Theory of propagation of elastic waves in a fluid saturated porous solid. II: higher frequency range. *J. Acoust. Soc. Am.* **28,** 179–191.

DREW, D. 1983 Mathematical modelling of two-phase flow. *A. Rev. Fluid Mech.* **15,** 261.

GIBSON, R. L. & TOKSÖZ, M. 1989 Viscous attenuation of acoustic waves in suspensions. *J. Acoust. Soc. Am.* **85,** 1925–1934.

HAMPTON, L. 1967 Acoustic properties of sediments. *J. Acoust. Soc. Am.* **42,** 882–890.

HARKER, A. & TEMPLE, J. 1988 Velocity and attenuation of ultrasound in suspensions of particles in fluids. *J. Phys. D.: Appl. Phys.* **21,** 1576–1588.

JACKSON, R. 1985 Hydrodynamic stability of fluid–particle systems. In *Fluidization*, Chap. 2 (Edited by DAVIDSON, J. F., CLIFT, R. & HARRISON, D.). Academic Press, New York.

JOHNSON, D. L., KOPLIK, K. & DASHEN, R. 1987 Theory of dynamic permeability and tortuosity in fluid-saturated porous media. *J. Fluid Mech.* **176,** 379–402.

KUSTER, G. & TOKSÖZ, M. 1986 Velocity and attenuation of seismic waves in two phase media: Part II. Experimental results. *Geophysics* **39,** 607–618.

LANDAU, L. D. & LIFSHITZ, E. M. 1982 *Fluid Mechanics*, 6th edn, p. 95. Pergamon Press, Oxford.

MAXWELL, J. C. 1881 *A Treatise on Electricity and Magnetism*, 2nd edn. Clarendon Press, Oxford.

ONODA, G. Y. & LINIGER, E. 1990 Random loose packings of uniform spheres and the dilatancy onset. *Phys. Rev. Lett.* **64,** 2727–2730.

SALIN, D. & SCHÖN, W. 1981 Acoustics of water saturated packed glass spheres. *J. Phys. Lett.* **42,** L477–L480.

TURNER, J. C. R. 1976 Two-phase conductivity: the electrical conductance of liquid-fluidized beds of spheres. *Chem. Engng Sci.* **31,** 487.

URICK, R. J. 1947 A sound velocity method for determining the compressibility of finely divided substances. *J. Acoust. Soc. Am.* **18,** 983–987.

URICK, R. J. 1948 The absorption of sound in suspensions of irregular particles. *J. Acoust. Soc. Am.* **20,** 283–289.

WALLIS, G. B. 1989 Inertial coupling in two-phase flow. *Multiphase Sci. Technol.* **5,** 239–361.

WATERMAN, P. & TRUELL, R. 1961 Multiple scattering of waves. *J. Math. Phys.* **2,** 512–540.